Journal of
Materials Chemistry B

Accepted Manuscript

This article can be cited before page numbers have been issued, to do this please use: N. Hao, J. Lu, M. chi, M. Xiong, Y. Zhang, R. Hua and K. Wang, *J. Mater. Chem. B*, 2019, DOI: 10.1039/C8TB03195A.

ROYAL SOCIETY OF CHEMISTRY

rsc.li/materials-b

View Article Online
DOI: 10.1039/C8TB03195A

A universal photoelectrochemical biosensor for dual microRNAs detection based on two CdTe nanocomposites

Nan Hao[a], Jinwen Lu[a], Mingji Chi[a], Meng Xiong[c], Ying Zhang[a], Rong Hua[a], Kun Wang[a,b,*]

[a]School of Chemistry and Chemical Engineering, Jiangsu University, Zhenjiang 212013, PR China

[b] Key Laboratory of Optic-electric Sensing and Analytical Chemistry for Life Science, Ministry of Education, College of Chemistry and Molecular Engineering, Qingdao University of Science and Technology, Qingdao 266042, PR China

[c] School of Biotechnology, Jiangsu University of Science and Technology, Zhenjiang 212018, PR China

*E-mail address: wangkun@ujs.edu.cn; Tel/Fax: +86 511 88791800

View Article Online
DOI: 10.1039/C8TB03195A

Abstract

Various diseases are closely related with simultaneous changes of multiple miRNAs expressions levels. It's of great significance to develop photoelectrochemical (PEC) biosensors for multiple miRNAs detection for both clinical diagnosis and biological mechanisms research. In this work we designed a novel PEC biosensor for simultaneous dual miRNAs detection for the first time. Two nanocomposites CdTe loaded on carbon nitrides nanosheets (CdTe-C_3N_4) with anodic photocurrent and CdTe loaded on 3D graphene hydrogel (CdTe-3DGH) with cathodic photocurrent were prepared and showed enhanced PEC performances. Photocurrents of the two nanocomposites can be clearly distinguished at corresponding critical voltage. Then probe DNA1 and DNA2 were combined with the CdTe-3DGH and CdTe-C_3N_4 NCs through covalent binding respectively. With the competition hybridization reaction between target miRNAs and the complementary DNA (cDNA), concentrations of miRNA141 and miRNA21 may be sensitively quantified by the respective photocurrents change. Compared with traditional PEC biosensors, this design didn't require any additional equipment and can provide a higher detection efficiency, which has a good universality and expansibility for the fabrication of multiplex PEC assays.

Keywords: photoelectrochemical; biosensor; dual targets; microRNA

View Article Online
DOI: 10.1039/C8TB03195A

1. Introduction

In recent years, photoelectrochemical (PEC) biosensors, as the combination of photoelectrochemistry and traditional electrochemical biosensing, have attracted considerable attentions with the advantages of easy operation, simple equipment and low cost.[1] Meanwhile, PEC sensing was regarded to have a better sensitivity compared with electrochemical sensing, which was attributed to that different forms of excitation signal (light signal) and detection signal (electric signal) brought a lower background noise.[2] A typical PEC biosensor was usually composed of two parts, the PEC active materials that conduct the light-electric energy conversion and the biological receptors that transduce the bio- or chemical information into the electric signal change through various signaling mechanisms.[3, 4]

MicroRNAs (miRNAs) are a kind of single-stranded, non-coding and small RNAs with about 19-23 nucleotides and there have been over 2000 species identified in human gene, which regulate cell proliferation, differentiation, apoptosis, tumorigenesis and a series of human physiological and pathological processes.[5-7] And the abnormally expression of miRNAs are related with a variety of diseases and could provide crucial messages for early diagnosis.[8, 9] However, quick, sensitive and quantitative detection of miRNAs is still a challenge due to short length, high sequence similarities among family members and low abundance.[10] Traditional methods including Northern blotting,[11, 12] microarray[13, 14] and reverse transcription real-time quantitative PCR (qRT-PCR).[15, 16] Although regarded as the golden standard, these methods suffer from large sample volumes, complex procedures or high cost.

View Article Online
DOI: 10.1039/C8TB03195A

etc. Until now, many different methods have been developed for miRNAs detection including fluorescence,[17-19] electrochemiluminescence[20, 21] and electrochemistry.[22,23] PEC analysis has good prospects for detecting miRNAs. For example, Dai's group developed a PEC biosensor for miRNA detection based on the surface plasmon resonance (SPR) of Au NPs enhanced resonant energy transfer (RET). The RET can efficiently amplify photocurrent generated by ZnSe-COOH nanoflakes (NFs). Then p19 protein that had specificity and high affinity for 21−23 bp double-stranded RNA was introduced to generate steric hindrance and dramatically quenched the photocurrent.[24, 25] Although possessing advantages of high sensitivity, simple operation and low cost, most present PEC biosensors can only detect a target at one detection.[26-31] Recent studies demonstrate that various diseases are closely related with simultaneous changes of multiple miRNAs expressions levels.[32, 33] So it's of great significance to develop PEC biosensors for multiple miRNAs detection for both clinical diagnosis and biological mechanisms research.[34, 35]

Multiplexed assays can improve detection efficiency, reduce test cost, save reagent consumption and sample volume. Despite many mechanisms have been developed, most PEC biosensors are still limited in the multiplex ability. Among these few works about PEC multiple assays, Hu's group reported a light addressing strategy that different probes were modified on different areas of a single electrode and multiple targets were detected one by one achieved by moving the light source from one sensing area to another.[36] Zhang et al. developed a PEC immunoassay for simultaneous dual cardiac markers detection with two specific enzymes tags to

View Article Online
DOI: 10.1039/C8TB03195A

differentiate the PEC signals.[37] Dai's group develop a potentiometric addressable PEC biosensor for simultaneous prostate-specific antigen and human interleukin-6 detection by adjusting applied voltage in the detection process. This method didn't require the movement of light source or specific enzymes, which has a good universality and expansibility for the fabrication of multiplex PEC assays.[38] Herein, in this work we designed a novel PEC biosensor for dual miRNAs detection for the first time. Two nanocomposites CdTe loaded on carbon nitrides nanosheets (CdTe-C_3N_4) with anodic photocurrent and CdTe loaded on 3D graphene hydrogel (CdTe-3DGH) with cathodic photocurrent were prepared and served as the PEC active materials. Photocurrents of the two nanocomposites can be clearly distinguished at corresponding critical voltage. With the competition hybridization reaction between target miRNAs and the complementary DNA (cDNA), concentrations of miRNA141 and miRNA21 may be sensitively quantified by the respective photocurrents change.

2. Experimental

2.1 Materials and reagents

1-Ethyl-3-(3-dimethylaminopropyl) carbodiimide hydrochloride (EDC), N-hydroxysuccinimide (NHS), $HAuCl{\cdot}4H_2O$ and 3-mercaptopropionic acid (MPA) were purchased from Sigma-Aldrich. Crystalline flake graphite was obtained from Qingdao Tianhe Graphite Co., Ltd. $CdCl_2{\cdot}2.5H_2O$, $NaBH_4$ (99%), Tellurium powder (Te, 99%) sodium dihydrogen phosphate ($NaH_2PO_4{\cdot}2H_2O$), disodium hydrogen phosphate ($Na_2HPO_4{\cdot}12H_2O$), ethanol and melamine were purchased from Sinopharm

View Article Online
DOI: 10.1039/C8TB03195A

Chemical Reagent Co. Ltd. Probe DNA1: 5′-NH_2-CCAT CTT TAC CAG ACA GTG TTA-3′; cDNA1: 5′-TAA CAC TGT CTG GTA AAG ATGG-SH-3′; microRNA 141: 5′-UAA CAC UGU CUG GUA AAG AUGG-3′. Probe DNA2: 5′-NH_2- TCAA CAT CAG TCT GAT AAG CTA-3′; cDNA2: 5′-TAG CTT ATC AGA CTG ATG TTGA-SH-3′; microRNA 21: 5′-UAG CUU AUC AGA CUG AUG UUGA-3′. microRNA 22: 5′-AAG CUG CCA GUU GAA GAA CUGU-3′, microRNA 200a: 5′-UAA CAC UGU CUG GUA ACG AUGU-3′. The above sequences were purchased Sangon Biotech Co., Ltd. All purchased reagents did not require further purified when used them. RNase-free ultrapure water was used throughout this study.

2.2 Apparatus

X-ray photoelectron spectroscopy (XPS) was conducted on a VG MultiLab 2000 system with a monochromatic Mg-Kα source operated at 20 kV. Scanning Electron Microscopy images were operated on the Hitachi S4800 scanning electron. Transmission Electron Microscopy images were conducted by the JEOL 2100 instrument. PEC measurements were operated by a CHI 760e electrochemical workstation (Shanghai Chenhua Instrument Co. Ltd., China) with a standard three-electrode cell system including the ITO as the working electrode, a saturated calomel electrode (SCE) as the reference electrode and a platinum (Pt) wire as the counter electrode. The whole PEC process was in pH 7.4 phosphate buffer solution (PBS) and a Xe lamp (PLS-SXM300/300UV, Beijing Perfect light) was utilized as the visible light source. Current-time (I–t) method was used in the whole PEC experiments.

View Article Online
DOI: 10.1039/C8TB03195A

2.3 Preparation of Au NPs and cDNA-coupled Au NPs

The Au NPs was prepared on the basis of the reported methods. In general, 0.6 mL of 0.1 M ice cold $NaBH_4$ was added into 20 mL 2.5×10^{-4} M $HAuCl_4$ solution under stirring. And the color of above solution turned into orange-red, indicating the AuNPs was formed. Next, the solution was stirred in ice cold water for 10 min and at room temperature for another 3 h until the color from orange-red to wine red. The prepared Au NPs was stored in 4 ℃ for further use.[39]

The synthesis of cDNA-coupled Au NPs (cDNA-Au) was as follows [39] : 50 μL of 50 mM Tris(2-carboxyethyl)phosphine（TCEP）was added in 500 μL of 1 μM mercapto (SH-) modified cDNA and the mixture was shaken for 2 h at room temperature to reduce disulfide bonds. Next, 490 μL Au NPs was mixed with the above mixture and shaken for 24 h and then 20μL of 0.1 M NaCl was added into the cDNA-Au solution with 5 minutes interval for five times respectively. The result solution was centrifuged at 15600 rpm for 30 min. Then the supernatant was removed and the precipitate was re-dispersed in 1 mL of 10 mM PBS (pH 7.4) containing 0.3 M NaCl.

2.4 The synthesis of CdTe-3DGH nanocomposites (NCs) and CdTe-C_3N_4 nanocomposites (NCs)

The synthesis steps of CdTe-3DGH NCs were described as follows. The preparation of graphene oxide was using the crystalline flake graphite through a modified Hummer's method.[40] The MPA-CdTe QDs was prepared in advance by a common method in previous reports.[41] Generally, 8 mg graphene oxide power was

View Article Online
DOI: 10.1039/C8TB03195A

dispersed in 5 mL ultrapure water with sonication for 1 h, then 2.5 mL CdTe QDs was added into the above suspension with stirring for 2 h. Next, the mixture was transferred to a 10 mL glass bottle and then placed in a 25 mL Teflon-lined autoclave with keeping 180 ℃ for 12 h. Finally, the product was cooled into room temperature and freeze dried for 24 h.

Similarly, the CdTe-C_3N_4 NCs were prepared through hydrothermal methods. C_3N_4 nanosheets were synthesized by a common approach in previous reports.[42] Concisely, 2 g melamine power was put in crucible and calcinated at 550 ℃ for 4 h under open air condition and the light yellow product was obtained after cooling down to room temperature. The CdTe-C_3N_4 NCs were synthesized by hydrothermal method. At the beginning, 25 mg C_3N_4 solid powder was dispersed in 10 mL ultra-pure water sonicated for 1 h. Next, 4 mL CdTe QDs solution was added into the above suspension with stirring for another 2 h. Finally, the mixture was transferred to a 25 mL Teflon-lined autoclave and heated at 180 ℃ for 12 h and the result product was freeze-dried for 24 h.

2.5 The fabrication of PEC biosensor

Firstly, the ITO electrodes were treated by boiling in ultrapure water containing 1 M NaOH for 30 min. And they were ultrasound in water and absolute ethyl alcohol for 30 min, respectively and dried under the infrared light before use. Secondly, 1 mg CdTe-3DGH NCs and CdTe-C_3N_4 NCs were respective dispersed into 1 mL ultrapure water with sonication for at least 1 h to obtain the suspension. 20 μL CdTe-3DGH NCs and CdTe-C_3N_4 NCs suspension were dropped onto two adjacent areas of one

View Article Online
DOI: 10.1039/C8TB03195A

ITO electrode with 0.5 cm^2 fixed area and then dried naturally overnight to fabricate a CdTe-3DGH/ CdTe-C_3N_4 modified ITO electrode. Thirdly, 10 μL of 10mM EDC and 20mM NHS were added on CdTe-3DGH and CdTe-C_3N_4 with incubation for 2 h and then rinsed with PBS, where the EDC played a coupling agent and NHS as an activator. Next 10 μL probe DNA1 and probe DNA2 were dropped on the CdTe-3DGH and CdTe-C_3N_4 and these ITO electrodes were at 4 ℃ for 12 h and then rinsed with PBS to remove the unbound probe DNA. Finally, 10 μL solution with different concentrations of target miRNA141 and miRNA21 was added on CdTe-3DGH and CdTe-C_3N_4 for 40 min and then rinsed with binding buffer. Afterwards, 10 μL cDNA-Au NPs solution was covered on the corresponding CdTe-3DGH/ CdTe-C_3N_4 electrodes and kept for 2 h and then these electrodes were washed with PBS and applied to PEC testing.

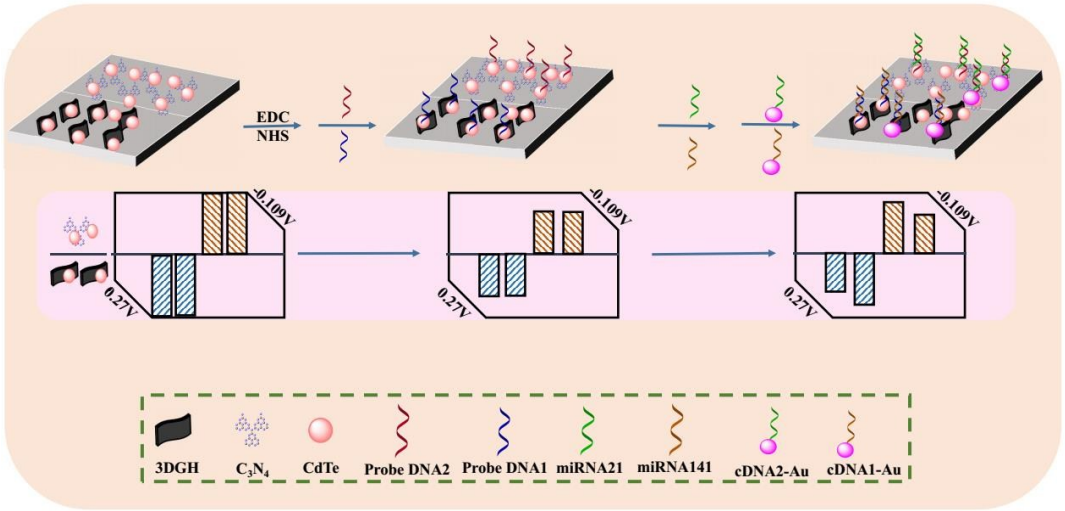

Scheme 1. The processes of constructing the photoelectrochemical biosensor for simultaneous dual microRNAs detection. Photocurrents of two nanocomposites CdTe-C_3N_4 and CdTe-3DGH can be clearly distinguished at corresponding critical voltage. Then probe DNA1 and DNA2 were combined with the CdTe-3DGH and CdTe-C_3N_4 NCs through covalent binding respectively. With

View Article Online
DOI: 10.1039/C8TB03195A

the competition hybridization reaction between target miRNAs and the complementary DNA (cDNA), concentrations of miRNA141 and miRNA21 may be sensitively quantified by the respective photocurrents change.

3. Result and Discussion

3.1 Schematic diagram of the experiment

The processes of the signal amplification PEC biosensor for dual miRNAs detection are illustrated in Scheme 1. At the beginning, the CdTe-3DGH and CdTe-C_3N_4 were modified onto two adjacent areas of one ITO electrode. When the bias voltage was set to the critical voltage of CdTe-3DGH (-0.109 V), the photocurrent from CdTe-3DGH was zero and the obtained anodic photocurrent was completely from CdTe-C_3N_4. Correspondingly, the cathodic photocurrent at 0.27 V (the critical voltage of CdTe-3DGH) was totally generated by CdTe-3DGH. So the photocurrents from two nanocomposites can be clearly distinguished by switching the bias voltage. Then two kinds of NH_2-probe DNA were modified on the electrode, the anodic and cathodic photocurrents of probe/CdTe-3DGH /CdTe-C_3N_4 decreased at -0.109 V and 0.27 V because of the enhanced steric hindrance. Next the target microRNA141 and mircoRNA21 were specifically binding to probe DNA and resulted in the further decrease of photocurrents. Afterwards, the two kinds of cDNA-Au NPs were dropped on the corresponding area and hybridized with unbound probe DNA and enhance the photocurrent due to the surface plasmon resonance of Au NPs.[43] The photocurrent values of different status were shown in Fig. S2. The modification of DNA probes caused the decrease of photocurrents. Andthe presence

View Article Online
DOI: 10.1039/C8TB03195A

of microRNA141 and mircoRNA21 further reduced the photocurrents. But when cDNA-Au NPs were added, an obvious enhancement effect could be observed. There were fewer unbound probe left for cDNA-Au NPs when the concentrations of targets were higher. So, the anodic and cathodic photocurrents were respectively inversely proportional to the concentration of microRNA141 and mircoRNA21. Therefore, a sensitive PEC biosensor for dual microRNAs detection was successfully constructed.

3.2 Characterization of CdTe-3DGH and CdTe-C_3N_4 NCs

In order to demonstrate the successful preparation of CdTe-3DGH and

View Article Online
DOI: 10.1039/C8TB03195A

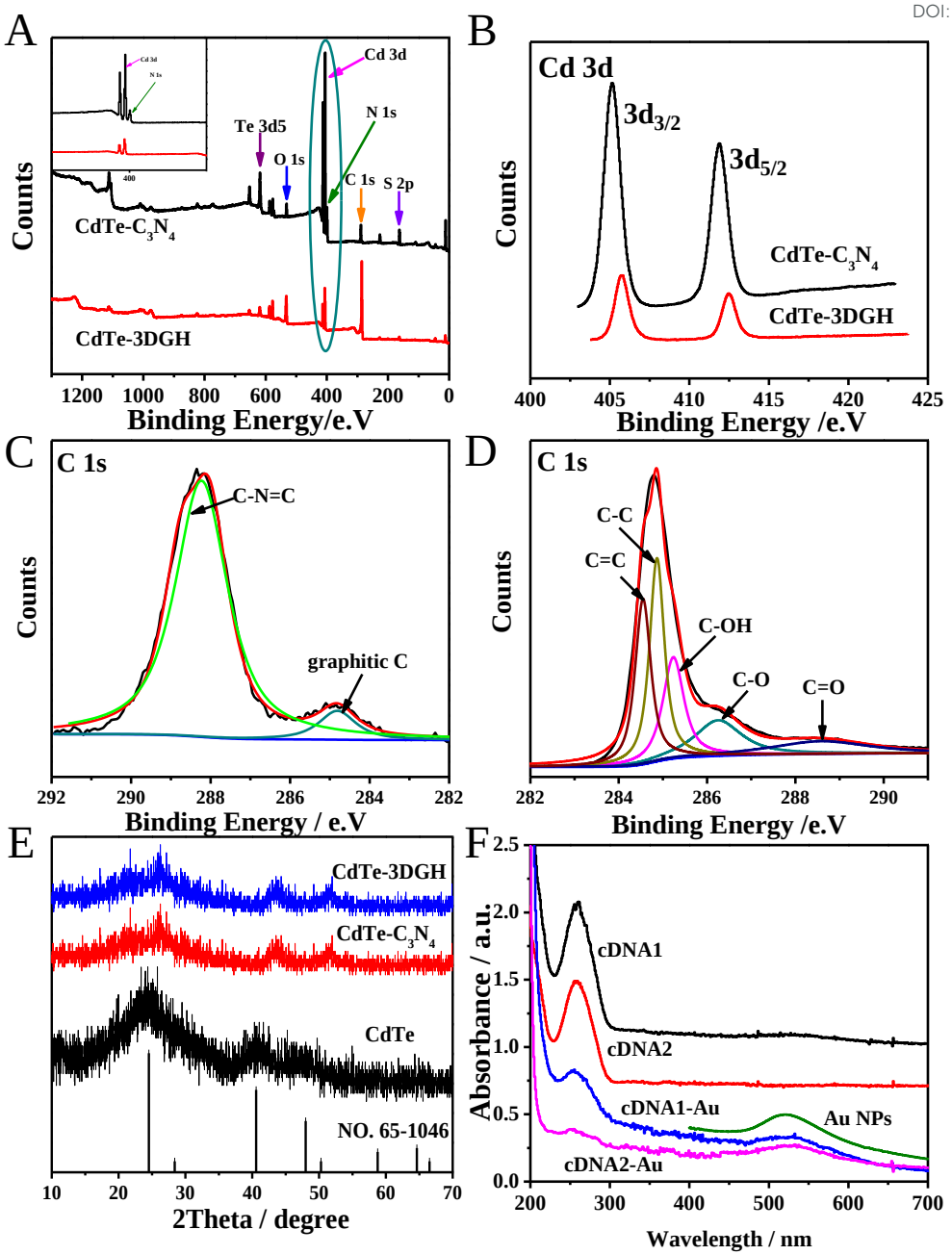

Fig. 1. XPS survey spectra of CdTe-3DGH and CdTe-C_3N_4 NCs (A). Cd 3d spectra of CdTe-3DGH and CdTe-C_3N_4 NCs (B). The high-resolution XPS spectra of C 1s region in CdTe-C_3N_4 NCs (C) and CdTe-3DGH NCs (D). XRD patterns of CdTe, CdTe-C_3N_4 NCs and CdTe-3DGH NCs (E). UV-vis absorption spectrum of different cDNA and cDNA-coupled Au NPs (F).

CdTe-C_3N_4, XPS, XRD, UV-vis, SEM and TEM data were presented. The XPS

View Article Online
DOI: 10.1039/C8TB03195A

images were shown in Fig. 1. In Fig. 1A, the peaks of Cd, Te, C, O and Cd, Te, C, N were clearly seen in CdTe-3DGH and CdTe-C_3N_4 NCs. Cd 3d showed two peaks (Cd $3d_{3/2}$ and Cd $3d_{5/2}$) in the two compounds at 405.2 and 411.8 eV through high-resolution scanning, indicating the existence of CdTe in the two nanocomposites (Fig. 1B).[44] The C 1s XPS spectrum of CdTe-C_3N_4 could be deconvoluted into two peaks at 288.2 and 284.8 eV (Fig. 1C), meaning the C-N=C and graphitic C type bonds.[45] The deconvoluted C 1s XPS spectrum of CdTe-3DGH showed five peaks at 284.5, 284.8, 285.2, 286.3, 288.6 corresponding to C=C, C-C, C-OH, C-O and C=O type bonds (Fig. 1D).[46, 47]

The X-Ray Diffraction (XRD) patterns of CdTe-3DGH and CdTe-C_3N_4 NCs were showed in Fig. 1E to discuss the phase structures. For bare MPA-CdTe QDs, several major diffraction peaks at 2θ=24.532, 40.598 and 48.008 were indexed to (111), (220) and (311) planes of cubic zinc blended structure of CdTe QDs (JCPDS File NO. 65-1046).[48] The positions of the diffraction peaks of CdTe-3DGH and CdTe-C_3N_4 NCs were the same as the pure MPA-CdTe QDs without any impurity peaks, which suggested the two composites hold high crystalline quality and the result compounds were successfully prepared. However, the diffraction peaks of GO and C_3N_4 were not detected due to the 3DGH and C_3N_4 sheets did not pile together and the peaks overlapped. The UV-vis absorption spectrum of cDNA and cDNA-coupled Au NPs were presented in Fig. 1F, it was clearly that cDNA1 and cDNA2 had the maximum absorption peak at 258±0.5 nm and the maximum absorption of pure Au

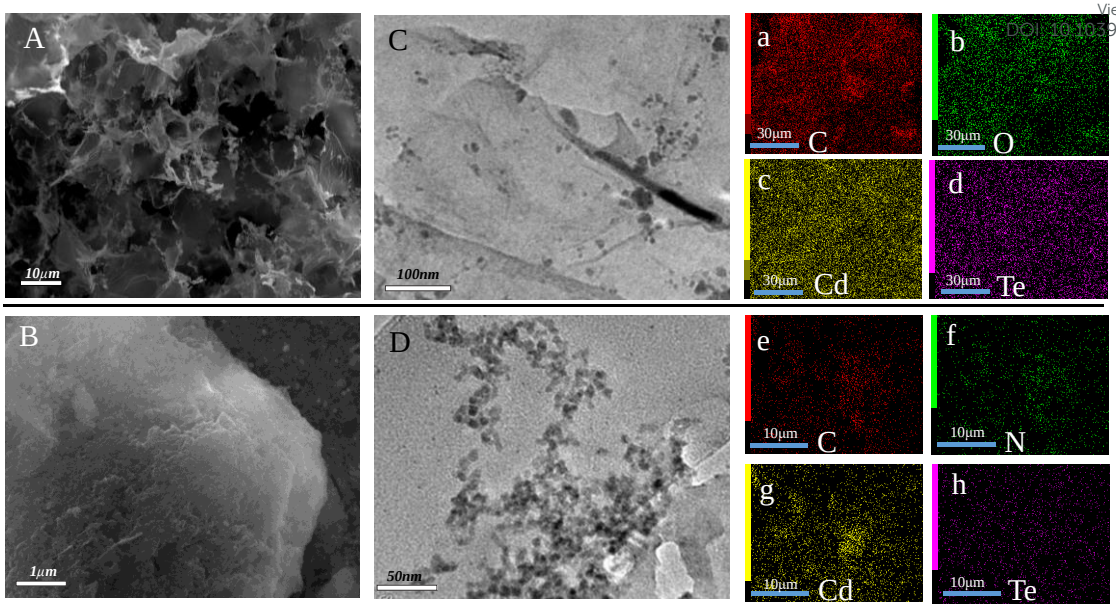

Fig. 2. SEM iamges of CdTe-3DGH (A) and CdTe-C_3N_4 (B). TEM images of CdTe-3DGH (C) and CdTe-C3N4 (D). Elemental mapping images (EMIs) of a) C, b) O, c) Cd and d) Te of CdTe-3DGH NCs and e) C, f) N, g) Cd and h) Te of CdTe-C_3N_4 NCs.

NPs at 522 nm. Two kinds of cDNA-coupled Au NPs had at 258 nm and 522 nm absorption peak, which proved that cDNA was fully connected to Au NPs.[49]

In order to further prove the successful preparation, SEM and TEM images were provided in Fig. 2. It was obvious that CdTe-3DGH (Fig. 2A) showed a cross-linked porous structure and CdTe-C_3N_4 (Fig. 2B) exhibited a stacked nanosheets structure. And the CdTe QDs were successfully loaded on the 3DGH (Fig. 2C) and C_3N_4 (Fig. 2D) nanosheets. Meanwhile, the Elemental mapping images (EMIs) demonstrated the presence of C, O, Cd, Te and C, N, Cd, Te elements in these two composites (Fig. 2a-h).

3.3 PEC performances and optimizations of CdTe-3DGH and CdTe-C_3N_4 NCs.

In Fig. 3A, the photocurrent of 60.0% CdTe QDs doped CdTe-3DGH NCs was 5 times that of pure CdTe QDs and higher other content (37.5%, 47.4%, 54.5%, 64.3%)

View Article Online
DOI: 10.1039/C8TB03195A

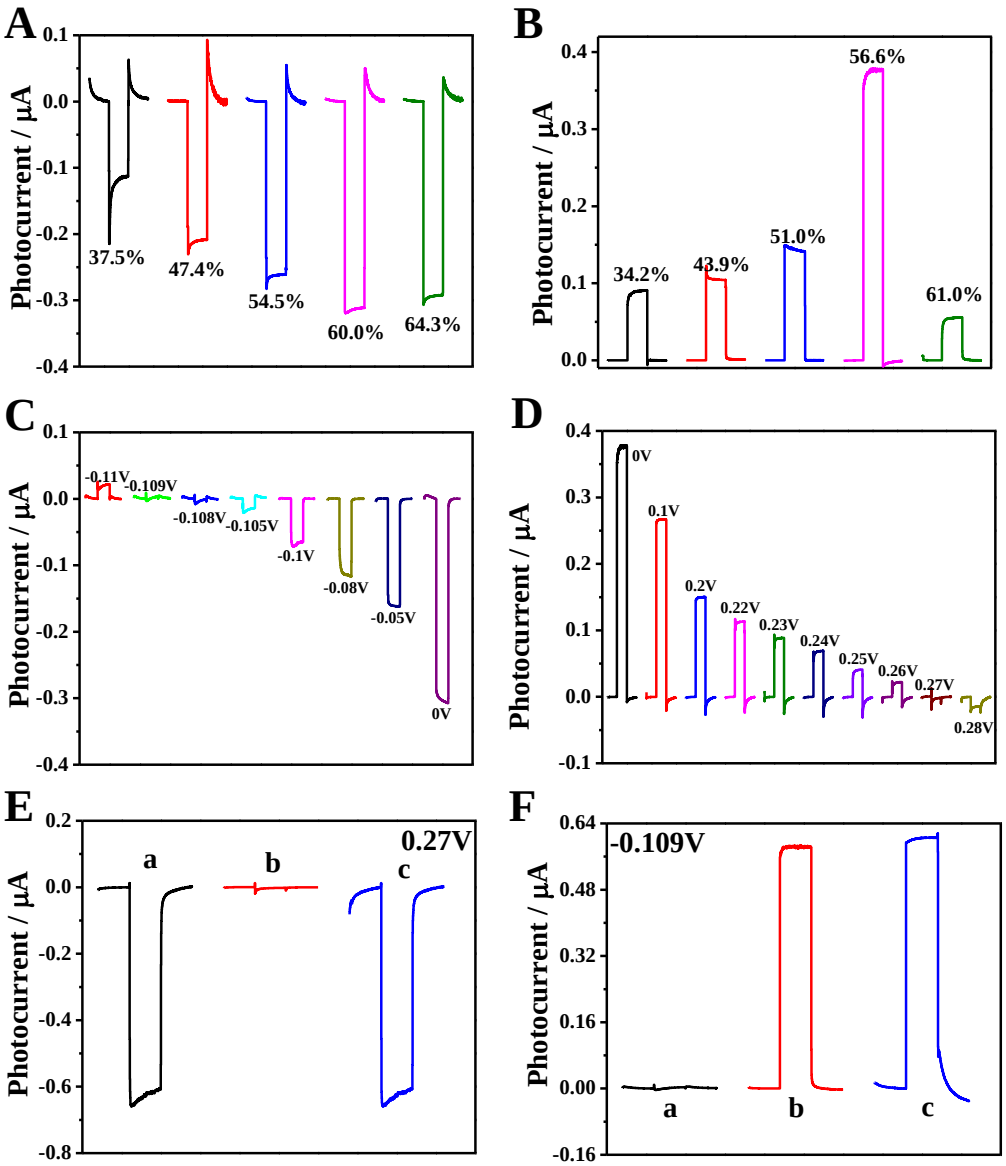

Fig. 3. The photocurrents of CdTe QDs doping CdTe-3DGH (A) and C_3N_4 nanosheets doping CdTe-C_3N_4 (B) with different ratios; the photocurrents of CdTe-3DGH (C) and CdTe-C_3N_4 (D) at different applied voltage; the photocurrents of CdTe-3DGH (a), CdTe-C_3N_4 (b), CdTe-3DGH/CdTe-C_3N_4 (c) at 0.27 V (E) and -0.109 V (F).

of CdTe-3DGH NCs because of the sensitization effect of 3DGH, suggesting a significant enhanced charge separation and transfer in the composite of CdTe-3DGH. When the CdTe QDs was 60.0%, the CdTe loading on the 3DGH nanosheets got the

View Article Online
DOI: 10.1039/C8TB03195A

saturation, the photocurrent of CdTe-3DGH tended to be stable. Similarly, different amounts of C_3N_4 doping in the CdTe-C_3N_4 NCs also brought changes of photocurrent as shown in Fig. 3B. The photocurrent increased with the increase of C_3N_4 (34.2-61.0%) and then decreased due to excessive C_3N_4 would hinder electron transfer.[50] Therefore, when 60.0% CdTe and 56.6% C_3N_4 was added, the photocurrent responses of CdTe-3DGH and CdTe-C_3N_4 were the maximum, indicating the optimal CdTe and C_3N_4 content and chosen for following experiment.

The photocurrent responses of CdTe-3DGH and CdTe-C_3N_4 at different applied voltage were investigated. As shown in Fig. 3C and 3D, it was clearly observed that the photocurrents were greatly affected by the bias voltage. And the photocurrents of CdTe-3DGH and CdTe-C_3N_4 decreased to zero at the corresponding critical voltage -0.109 V (CdTe-3DGH) and 0.27 V (CdTe-C_3N_4). At 0.27 V, the cathodic photocurrents of CdTe-3DGH (a) modified electrode and CdTe-3DGH/CdTe-C_3N_4 dual modified electrode (c) were almost the same (Fig. 3E). Similarly, there was no difference between the anodic photocurrents of CdTe-C_3N_4 (b) and CdTe-3DGH/CdTe-C_3N_4 (c) at -0.109 V (Fig. 3F), which indicated photocurrents from these two nanocomposites modified one ITO electrode can be well discriminated.

3.4 PEC behaviors of modified ITO electrodes and PEC Biosensing for MiRNAs

Optimizing the experimental conditions played an essential role throughout the experiment. The optimization of probe DNA concentration (Fig. S1A) and the binding time between the target and probe DNA (Fig. S1B) were displayed in supporting information. Then this biosensor was applied for simultaneous detection of

View Article Online
DOI: 10.1039/C8TB03195A

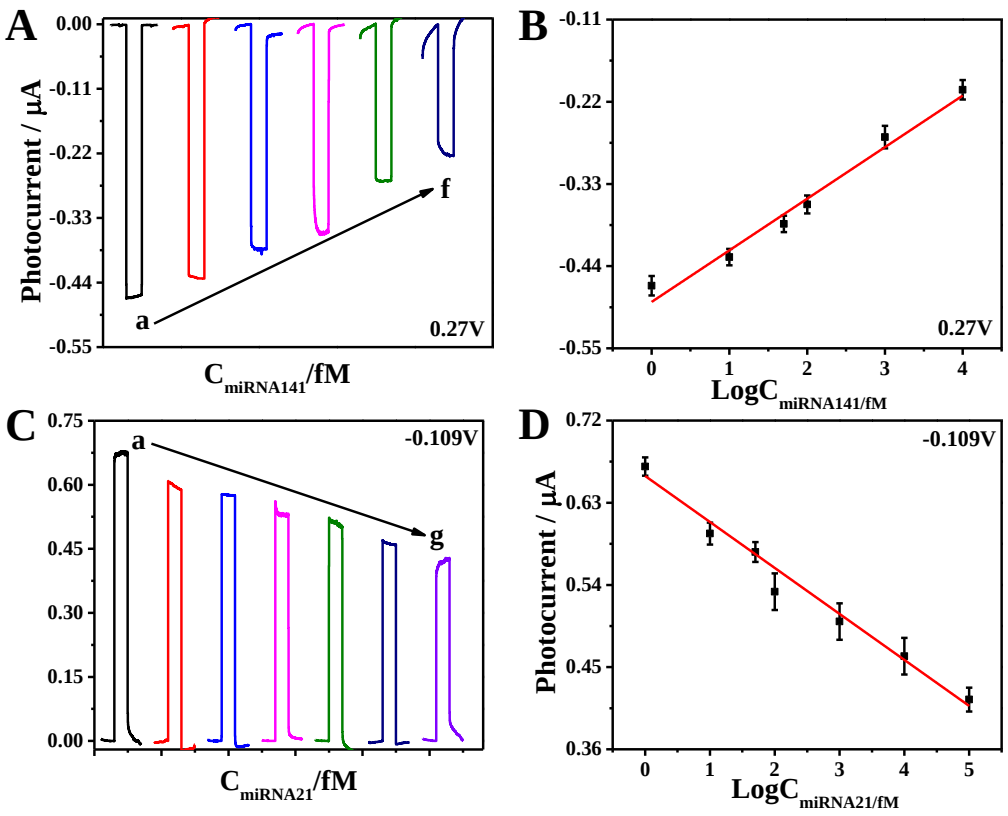

Fig. 4. The photocurrents of CdTe-3DGH/CdTe-C3N4 electrodes at 0.27 V in the presence of 1, 10, 50, 100, 1000, 10^4 fM microRNA141 (A) and at -0.109 V in the existence of 1, 10, 50, 100, 1000, 10^4, 10^5 fM microRNA21 (C). The corresponding linear calibration curves of microRNA141 (B) and 21 (D).

miRNA141 and miRNA21 with concentrations from 1.0 fM to $1.0*10^4$ fM. The corresponding cathodic and anodic photocurrents were revealed in Fig. 4A and 4C. It was apparent that the photocurrents decreased when targets concentrations increased. Due to the SPR of Au NPs can enhance light absorption and photocurrent transfer efficiency, the binding of cDNA-Au with probe would cause the increase of photocurrent. Because of the competition hybridization reaction between target miRNAs and the cDNA, more targets in the sample lead to fewer Au NPs bound on the electrode. Therefore, the cathodic and anodic photocurrent values were inversely

View Article Online
DOI: 10.1039/C8TB03195A

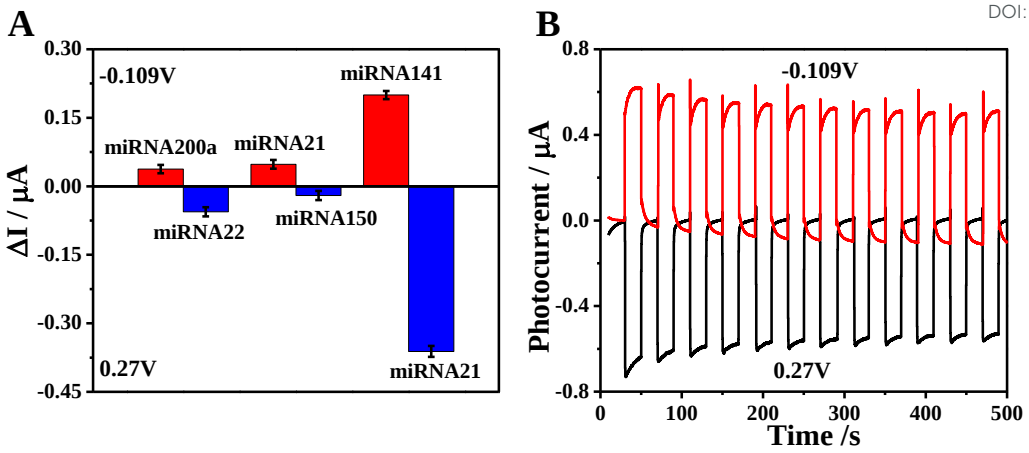

Fig. 5. Photocurrent responses of CdTe-3DGH/CdTe-C_3N_4 electrode at -0.109 V and 0.27 V (A). $\Delta \boldsymbol{I}_{-0.109V}$ ($\boldsymbol{I}$-$\boldsymbol{I}_0$, $\boldsymbol{I}$ was photocurrent towards different miRNAs; $\boldsymbol{I}_0$ was the phohocurrent of CdTe-3DGH/CdTe-C_3N_4/probe) in the presence of 1 pM miRNA141, 200 pM miRNA200a and miRNA21 and $\Delta \boldsymbol{I}_{0.27V}$ was faced to 1 pM miRNA21, 200 pM miRNA22 and miRNA150 (B).

proportional to logarithmic values of the concentrations with the linear range for 1.0 to 1.0*10^4 fM miRNA141 (R^2=0.972) and 1.0 to 1.0*10^5 fM miRNA21 (R^2=0.982), respectively (Fig. 4B and 4D). The detection performance was compared with previous biosensors for dual miRNAs detection and showed satisfied sensitivity (Table S1).

3.5 Selectivity and Stability of PEC biosensor

Selectivity and stability are always used to evaluate the detection performance. The selectivity of this PEC biosensor was assessed by comparing the $\Delta \boldsymbol{I}_{-0.109V}$ and $\Delta \boldsymbol{I}_{0.27V}$ in the presence of other similar miRNAs. It was significant that the $\Delta \boldsymbol{I}_{-0.109V}$ of miRNA141 and $\Delta \boldsymbol{I}_{0.27V}$ of miRNA21 were the maximal in Fig. 5A, which attributed to the specific binding between the miRNA141 or miRNA21 and probe DNA1 or 2. Simultaneously, as shown in Fig. 5B, the stability of this biosensor was measured

View Article Online
DOI: 10.1039/C8TB03195A

through comparing the anodic (-0.109 V) and cathodic (0.27 V) photocurrents produced by the Xe lamp switched on interval of 30s and repeated about 12 times. There was no obvious change of photocurrents, which suggested this biosensor had superior stability.

3.6 Real sample detection

In order to further confirm the practicality of designed PEC biosensor for miRNAs detection in real samples, different concentrations of targets were added into human blood serum obtained from affiliated hospital of Jiangsu university through standard addition method. The final results were displayed in Table 1, the recoveries of this method were ranging from 98.8% to 102.7% for microRNA141 and 98.5% to 102.9% for microRNA21. Meanwhile, the relative standard deviation (RSD) were from 3.5% to 7.1% and 2.1% to 6.9% respectively. The result meant this PEC biosensor had good stability and reproducibility in real biological samples.

Table 1. The recovery of the proposed biosensor array in human serum (n=3).

Samples	miRNA-141 (fM)			miRNA-21 (fM)		
	1	2	3	1	2	3
Added	15	150	1500	15	150	1500
Found	15.41	151.81	1482	14.77	151.2	1544.2
RSD (%)	6.6	7.1	3.5	2.1	3.6	6.9
Recovery (%)	102.7	101.2	98.8	98.5	100.8	102.9

View Article Online
DOI: 10.1039/C8TB03195A

4. Conclusion

In summary, a sensitive and novel PEC biosensor for dual microRNAs detection has been successfully constructed. CdTe-3DGH and CdTe-C_3N_4 were prepared through a facile hydrothermal method and served as the PEC active materials. Based on the potentiometric addressable principle, the cathodic photocurrent generated by CdTe-3DGH and anodic photocurrent generated by CdTe-C_3N_4 can be well distinguished by adjusting the bias voltage after modified onto one ITO electrode. Through the competition hybridization reaction with probe DNA, the concentrations of target miRNAs would affect the binding of cDNA-coupled Au NPs on the electrode. Due to the SPR of Au NPs can enhance light absorption and photocurrent transfer efficiency, the binding of cDNA-Au would cause the increase of photocurrent. Therefore, the cathodic and anodic photocurrent values were inversely proportional to the concentrations of miRNA141and miRNA21 respectively. Compared with traditional PEC biosensors, this photoelectrochemical biosensor can improve detection efficiency, reduce test cost, save reagent consumption and sample volume, which has excellent prospects for clinical diagnosis and biological mechanisms research.

Supporting information

The Supporting Information is available free of charge on the RSC Publications website. Preparation of materials and sensors, characterization of nanomaterials, comparison of the as-prepared methods with those reported in the literatures were provided in supplementary materials.

View Article Online
DOI: 10.1039/C8TB03195A

Acknowledgments

This work was supported by National Natural Science Foundation of China (Nos. 21876068, 21505055, 21705059 and 21675066), Natural Science Foundation of Jiangsu Province (No.BK20150486), China Postdoctoral Science Foundation funded project (2017M621652), Special Foundation of China Postdoctoral (2018T110456), Postdoctoral Science Foundation funded project of Jiangsu province (1701075C), Foundation of Jiangsu University (15JDG145), and the Foundation of Key Laboratory of Sensor Analysis of Tumor Marker, Ministry of Education, Qingdao University of Science and Technology (No. SATM201807), Jiangsu Provincial Engineering Laboratory for Advanced Materials of Salt Chemical Industry (SF201703).

References

1. B. Zhang and L. H. Guo, ***Biosensors & Bioelectronics***, 2012, **37**, 112-115.
2. G. L. Wang, J. X. Shu, Y. M. Dong, X. M. Wu, W. W. Zhao, J. J. Xu and H. Y. Chen, ***Analytical Chemistry***, 2015, **87**, 2892-2900.
3. W. W. Zhao, J. Wang, J. J. Xu and H. Y. Chen, ***Chemical Communications***, 2011, **47**, 10990-10992.
4. D. Chen, H. Zhang, X. Li and J. Li, ***Analytical Chemistry***, 2010, **82**, 2253-2261.
5. P. Landgraf, M. Rusu, R. Sheridan, A. Sewer, N. Iovino, A. Aravin, S. Pfeffer, A. Rice, A. O. Kamphorst and M. Landthaler, ***Cell***, 2007, **129**, 1401-1414.
6. M. V. Iorio, M. Ferracin, C. G. Liu, A. Veronese, R. Spizzo, S. Sabbioni, E.

Magri, M. Pedriali, M. Fabbri and M. Campiglio, ***Cancer Research***, 2005, **65**, 7065-7070.

7. H. Liu, J. Fan, W. Liu, C. Tong, Z. Xie, R. Deng and X. Long, ***Analytical Methods***, 2018, **10**, 5834-5841.
8. A. Chen, G. F. Gui, Y. Zhuo, Y. Q. Chai, Y. Xiang and R. Yuan, ***Analytical Chemistry***, 2015, **87**, 6328-6334.
9. R. Deng, K. Zhang and J. Li, ***Accounts of Chemical Research***, 2017, **50**, 1059-1068.
10. M. Baker, ***Nature Methods***, 2010, **7**, 687-692.
11. É. Várallyay, J. Burgyán and Z. Havelda, ***Nature Protocols***, 2008, **3**, 190-196.
12. A. Válóczi, C. Hornyik, N. Varga, J. Burgyán, S. Kauppinen and Z. Havelda, ***Nucleic Acids Research***, 2004, **32**, e175-e175.
13. J. M. Thomson, J. Parker, C. M. Perou and S. M. Hammond, ***Nature Methods***, 2004, **1**, 47-53.
14. N. Yang, S. Kaur, S. Volinia, J. Greshock, H. Lassus, K. Hasegawa, S. Liang, A. Leminen, S. Deng and L. Smith, ***Cancer Research***, 2009, **68**, 10307-10314.
15. J. Li, B. Yao, H. Huang, Z. Wang, C. Sun, Y. Fan, Q. Chang, S. Li, X. Wang and J. Xi, ***Analytical Chemistry***, 2009, **81**, 5446-5451.
16. K. Lao, N. L. Xu, V. Yeung, C. Chen, K. J. Livak and N. A. Straus, ***Biochemical & Biophysical Research Communications***, 2006, **343**, 85-89.
17. L. Liang, F. Lan, X. Yin, S. Ge, J. Yu and M. Yan, ***Biosens Bioelectron***, 2017, **95**, 181-188.

View Article Online
DOI: 10.1039/C8TB03195A

18. R. Huang, Y. Liao, X. Zhou, Y. Fu and D. Xing, ***Sensors and Actuators B: Chemical***, 2017, **247**, 505-513.

19. R. Deng, K. Zhang, L. Wang, X. Ren, Y. Sun and J. Li, ***Chem***, 2018, **4**, 1373-1386.

20. X. Feng, N. Gan, H. Zhang, T. Li, Y. Cao, F. Hu and Q. Jiang, ***Biosensors & Bioelectronics***, 2016, **75**, 308-314.

21. L. Peng, P. Zhang, Y. Chai and R. Yuan, ***Anal Chem***, 2017, **89**, 5036-5042.

22. D. Zeng, Z. Wang, Z. Meng, W. Peng, L. San, W. Wei, A. Aldalbahi, L. Li, J. Shen and X. Mi, ***Acs Appl Mater Interfaces***, 2017, **9,** 24118-24125.

23. W. Zhu, X. Su, X. Gao, Z. Dai and X. Zou, ***Biosensors & Bioelectronics***, 2014, **53**, 414-419.

24. W. Tu, H. Cao, Z. Long, J. Bao, X. Liu and Z. Dai, ***Analytical Chemistry***, 2016, **88**,10459-10465

25. W. Lu, Y. Jin, G. Wang, D. Chen and J. Li, ***Biosensors and Bioelectronics***, 2008, **23**, 1534-1539.

26. Q. Shen, L. Han, G. Fan, J. R. Zhang, L. Jiang and J. J. Zhu, ***Anal Chem***, 2015, **87**, 4949-4956.

27. T. Hou, W. Li, X. Liu and F. Li, ***Anal Chem***, 2015, **87**, 11368-11374.

28. R. Xu, Y. Jiang, L. Xia, T. Zhang, L. Xu, S. Zhang, D. Liu and H. Song, ***Biosensors & Bioelectronics***, 2015, **74**, 411-417.

29. M. Zhao, G. C. Fan, J. J. Chen, J. J. Shi and J. J. Zhu, ***Anal Chem***, 2015, **87**, 12340-12347.

View Article Online
DOI: 10.1039/C8TB03195A

30. X. Tang, R. Deng, Y. Sun, X. Ren, M. Zhou and J. Li, ***Analytical Chemistry***, 2018, **90**, 10001-10008.

31. R. Deng, K. Zhang, Y. Sun, X. Ren and J. Li, ***Chemical Science***, 2017, **8**, 3668-3675.

32. B. C. Yin, Y. Q. Liu and B. C. Ye, ***Journal of the American Chemical Society***, 2012, **134**, 5064-5067.

33. W. Lu, G. Wang, Y. Jin, X. Yao, J. Hu and J. Li, ***Applied Physics Letters***, 2006, **89**,177-181.

34. Q. Tian, Y. Wang, R. Deng, L. Lin, Y. Liu and J. Li, ***Nanoscale***, 2015, **7**, 987-993.

35. R. Deng, L. Tang, Q. Tian, Y. Wang, L. Lin and J. Li, ***Angewandte Chemie***, 2014, **126**, 2421-2425.

36. J. Wang, Z. Liu, C. Hu and S. Hu, ***Anal Chem***, 2015, **87**, 9368-9375.

37. N. Zhang, Z. Y. Ma, Y. F. Ruan, W. W. Zhao, J. J. Xu and H. Y. Chen, ***Analytical Chemistry***, 2016, **88**, 1990-1994.

38. H. Dai, S. Zhang, Z. Hong and Y. Lin, ***Anal Chem***, 2016, **88**, 9532-9538.

39. Z. Y. Ma, F. Xu, Y. Qin, W. W. Zhao, J. J. Xu and H. Y. Chen, ***Analytical Chemistry***, 2016, **88**, 4183-4187.

40. S. Gilje, S. Han, M. Wang, K. L. Wang and R. B. Kaner, ***Nano Lett.***, 2007, **7**, 3394-3398.

41. K. Zhang, Q. Mei, G. Guan, B. Liu, S. Wang and Z. Zhang, ***Analytical Chemistry***, 2010, **82**, 9579-9586.

View Article Online
DOI: 10.1039/C8TB03195A

42. W. Yin-Zhu, H. Nan, F. Qiu-Mei, S. Hai-Wei, X. Jing-Juan and C. Hong-Yuan, ***Biosensors & Bioelectronics***, 2016, **77**, 76-82.

43. M. Wang, H. Yin, N. Shen, Z. Xu, B. Sun and S. Ai, ***Biosensors & Bioelectronics***, 2014, **53**, 232-237.

44. B. J. Kowalski, B. A. Orlowski and J. Ghijsen, ***Surf. Sci,*** 1998, **412**, 544-554.

45. L. Ye, J. Liu, Z. Jiang, T. Peng and L. Zan, ***Applied Catalysis B Environmental***, 2013, **142-143**, 1-7.

46. D. Wang, M. Zhang, Z. Chen, H. Li, A. Chen, X. Wang and J. Yang, ***Sensors and Actuators B: Chemical***, 2017, **250**, 533-542.

47. N. Hao, X. Zhang, Z. Zhou, J. Qian, Q. Liu, S. Chen, Y. Zhang and K. Wang, ***Sensors and Actuators B: Chemical***, 2017, **250**, 476-483.

48. B. Bajorowicz, J. Nadolna, W. Lisowski, T. Klimczuk and A. Zaleska-Medynska, ***Applied Catalysis B Environmental***, 2017, **203**, 452-464.

49. Y. C. Zhu, F. Xu, N. Zhang, W. W. Zhao, J. J. Xu and H. Y. Chen, ***Biosensors & Bioelectronics***, 2017, **91**, 293-298.

50. Y. Zheng, L. Lin, B. Wang and X. Wang, ***Cheminform***, 2015, **54**, 12868-12884.

View Article Online
DOI: 10.1039/C8TB03195A

For TOC only

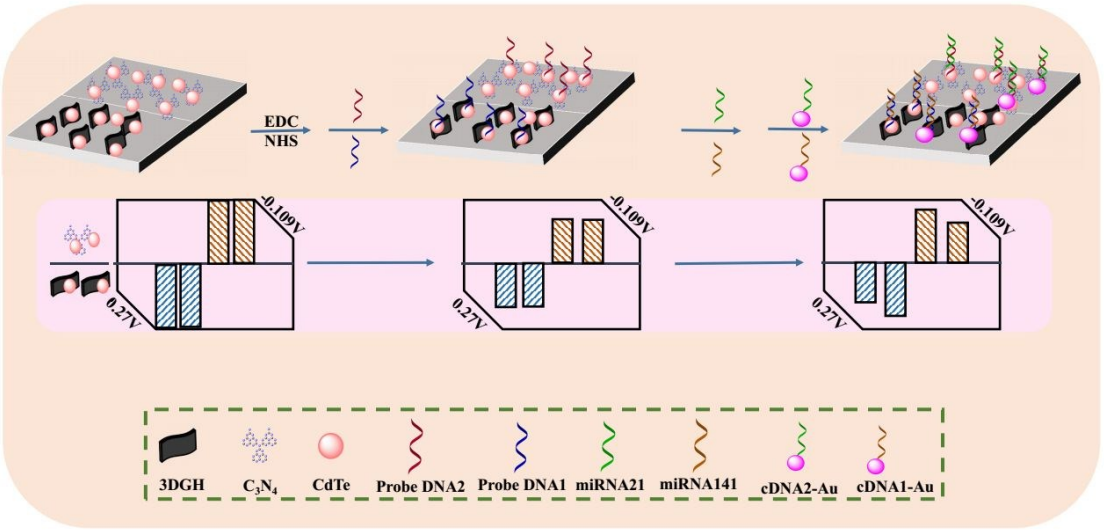

A universal photoelectrochemical biosensor for dual microRNAs detection has been successfully developed.